

Research Article

The Physical Modeling Analysis of Fate and Transport of Silver Nanoparticles Dispersed by Water Flow

Achmad Syafiuddin ¹, Salmiati Salmiati ², Mohamad Ali Fulazzaky ^{3,4},
Dedy Dwi Prastyo ⁵, Raj Boopathy ⁶, and Mu. Naushad ⁷

¹Department of Public Health, Universitas Nahdlatul Ulama Surabaya, Surabaya 60237, East Java, Indonesia

²Department of Water and Environmental Engineering, Faculty of Engineering, Universiti Teknologi Malaysia, Johor Bahru 81310, Malaysia

³School of Postgraduate Studies, University of Djuanda, Jalan Tol Ciawi No. 1, Ciawi, Bogor 16720, Indonesia

⁴Directorate General of Water Resources, Ministry of Public Works and Housing, Jalan Pattimura No. 20, Jakarta 12110, Indonesia

⁵Department of Statistics, Institut Teknologi Sepuluh Nopember, Surabaya 60111, Indonesia

⁶Department of Biological Sciences, Nicholls State University, Thibodaux, LA 70310, USA

⁷Department of Chemistry, College of Science, King Saud University, P.O. Box 2455, Riyadh 11451, Saudi Arabia

Correspondence should be addressed to Achmad Syafiuddin; achmadsyafiuddin@unusa.ac.id and Mohamad Ali Fulazzaky; fulazzaky@unida.ac.id

Received 13 September 2021; Accepted 20 October 2021; Published 2 November 2021

Academic Editor: Liviu Mitu

Copyright © 2021 Achmad Syafiuddin et al. This is an open access article distributed under the Creative Commons Attribution License, which permits unrestricted use, distribution, and reproduction in any medium, provided the original work is properly cited.

The release of silver nanoparticles (AgNPs) from consumer products into an environment has become a central issue for many countries. Despite that the fate and behaviors of AgNPs incorporated into a wastewater have been investigated by building a model of wastewater treatment process, the transport and retention behaviors of AgNPs influenced by the water flow in a river must be understood. The physical model of simulated river to mimic a natural flow of river was proposed to investigate the behaviors of AgNP transport in the river. The results showed that the large amount of AgNPs deposited on the riverbed as Ag sediment with only 1.26% of AgNPs remained in the water flow. The elemental content of Ag freely dispersed across the riverbed increases from the upstream to downstream area of the simulated river. Verification of the spatial distribution of Ag dispersed along the water flow may contribute to a better understanding of the fate and transport of AgNPs in the aquatic environment.

1. Introduction

Silver nanoparticles (AgNPs) that are usually considered as an engineered nanomaterial have been used in a wide range of industrial applications due to the physicochemical properties, and antimicrobial effects of AgNPs could be effective against many types of microorganisms [1, 2]. Antibacterial properties of AgNPs against the bacterial strains of *Staphylococcus aureus* and *Escherichia coli* have been analyzed to determine the minimum inhibitory concentration [3]. The release of wasted consumer products into the environment can result in the contamination of water

bodies with the various concentrations of AgNPs and has the potential to adversely affect aquatic organisms [4]. The toxicity effects on aquatic organisms could be dependent on the characteristic features of AgNPs and the types of living organisms. Spherical AgNPs having a size of 10–20 nm can defect the fin regeneration and penetrate into the cell organelles and nucleus of the zebrafish [5], while the toxicity of AgNPs in the zebrafish may lead to a reduction of silver uptake and fish mortality [6]. AgNP toxicity to certain freshwater fish species mediated by dissolved silver can bind the cultured fish gill cells leading to decrease in the tolerance of such freshwater fish to hypoxic conditions [7] and to an

increase in the susceptibility to oxidative stress in the gills of brown trout [8]. The toxicity of AgNP-contaminated water in freshwater fish can lead to an increase in the vulnerability of the brain antioxidant enzyme system of the Nile tilapia and redbelly tilapia [9]. The toxic effect of AgNPs on ray-finned fish can increase the level of liver glycogen and leads to an enlargement of fish muscle fibers [10].

The moving water in a river of carrying AgNPs may disperse the particles of sediment released from the riverbed and creates a space devoid of downstream-flowing water from the downstream side of AgNPs' entry point. The fate and transport of AgNPs in a river can not only be followed according to the laminar flow of water but also must be monitored in complex environmental relevant conditions [11]. Turbulence flow of water could not only disperse the sediment particles but can also modulate a settling velocity of AgNPs on the riverbed. The investigation of AgNP distribution may be bearing on the transportation of sediment released from the riverbed and detritus in terms of discharge and slope. The modeling of AgNPs transported by the flow of wastewater passed through the channel of wastewater treatment plant (WWTP) showed that the typical facility of WWTP designed to remove the excessive amount of AgNPs is effective with an approximately 1% loss of AgNPs from the channel system [12]. The behavior of AgNPs transported in the pilot WWTP fed with municipal wastewater has been investigated to show that the physical and chemical changes of AgNPs adsorbed to the wastewater biosolids control the fate, toxicity, and bioavailability of AgNPs with approximately 2.5% loss of AgNPs into the environment [13]. The removal of citrate AgNPs in the simulated wastewater treatment processes shows over 90% of AgNPs remained in the wastewater after the primary clarification unit entering the subsequent treatment units can remove more AgNPs from wastewater with approximately 6% of AgNPs remained in effluent flowing into the environment [14].

A number of studies have been conducted in the context of modeling the WWTP processes to investigate the fate and behaviors of AgNPs in wastewater [13, 15], which probably have distinctive behaviors of water compared to the natural flow of a river. This study aims to investigate the mechanism of AgNP transport that both the water flow and riverbed of the river system play a role in the understanding of retention and mobility mechanisms of AgNPs in the natural flow of water. The study was limited to the use of a simulated river system with a slope of 5.7° aimed to mimic the natural flow of water at flow rate of 0.8 L/min to advance an understanding of the fate and transport of AgNPs material in the environment.

2. Materials and Methods

2.1. Materials. Silver nitrate (AgNO_3) originally coming from the QRëC company (QRëC, New Zealand) was used as a source of Ag^+ for the synthesis of AgNPs. The leaves of *Muntingia calabura* collected from the surrounding area of Universiti Teknologi Malaysia were used as a natural reducing agent in the formation of AgNPs. A filter of the Whatman® Nylon membrane with 0.45 μm pore size

originally purchased from Sigma-Aldrich (Missouri, United States) was used for the filtration of *Muntingia calabura* leaves extract. The ultrapure water processed by the arium® pro VF Ultrapure Water System (Sartorius Malaysia Sdn Bhd, Kuala Lumpur, Malaysia) was used to prepare the solution for the synthesis of AgNPs.

2.2. AgNP Synthesis. On the one side of AgNP solution synthesis, approximately 18 g of fresh *Muntingia calabura* leaves were washed with running tap water and then with ultrapure water and then put into 200 mL ultrapure water in a 500 mL Erlenmeyer flask and boiled on a hot plate at 250°C for 30 min. The solution containing the *Muntingia calabura* leaves extract was cooled at room temperature and then filtered using the nylon membrane to obtain the pure *Muntingia calabura* leaf extract and then kept in the fridge for the next use. On the other side, 2.55 g of AgNO_3 was diluted into 100 mL ultrapure water in an Erlenmeyer flask of 500 mL to prepare the solution of 0.15 M AgNO_3 . The synthesis of AgNPs solution was performed by mixing 100 mL pure *Muntingia calabura* leaf extract with 100 mL 0.15 M AgNO_3 solution and then left in the laboratory at room temperature for 24 h. The physiochemical properties of AgNPs are listed in Table 1.

2.3. Simulated River System. The simulated river system (see Figure 1) consisting of an influent, water storage tank, river channel, effluent tank, AgNPs solution tank, and electric pump was used for running the experiment. The rate of influent flow into the water storage tank with its dimension of 59 × 43 × 39 cm^3 was controlled using a valve. A channel using the PVC gutter with its length of 600 cm was installed on a slope distance of 5.7° as the simulated river. Clay soil collected from an area surrounding the Universiti Teknologi Malaysia was adhered to the bottom of simulated river with an average width of 3 cm to mimic the natural conditions of a river. A simulated river was very susceptible to the spread of AgNPs affected by running water when clay soil was in direct contact with flowing water. This may represent the natural function of a river to carry AgNPs from the upstream to downstream area of the simulated river and allows an interaction between AgNPs and soil particles [17]. Any volume of water passed through the simulated river was stored in an effluent storage tank. The design parameters of simulated river system are depicted in Table 2.

2.4. Experimental Setup and Sampling Procedures. The storage tank was filled with an influent of the tap water to give it sufficient volume to flow into the simulated river and regulated by a control valve. The continuous feeding of the influent leading to an overflow of the water storage tank flowing into the simulated river was controlled at the flow rate of 0.8 L/min, allowing until it reached at a steady-state condition. A water quality checker of the YSI Pro Plus Multiparameter Water Quality Meter was installed at both the storage and effluent tanks of the simulated river system to monitor the water quality parameters of temperature, pH,

TABLE 1: Physiochemical properties of AgNPs [16].

Parameter	Unit	Value
Molecular weight	g/mol	107.87
Melting point	°C	961.78
Boiling point	°C	2162
Bulk density	g/cm ³	0.312
Size range	nm	1–100
Specific surface area	m ² /g	5.37
Crystal structure		Cubic
Poisson's ratio		0.37
Thermal expansion	$\mu\text{m}\cdot\text{m}^{-1}\text{K}^{-1}$	(25°C) 18.9
Vickers hardness	MPa	251
Young's modulus	GPa	83
Covalent radius	Å	1.53
van der Waals radius	Å	1.72
α line	keV	2.98

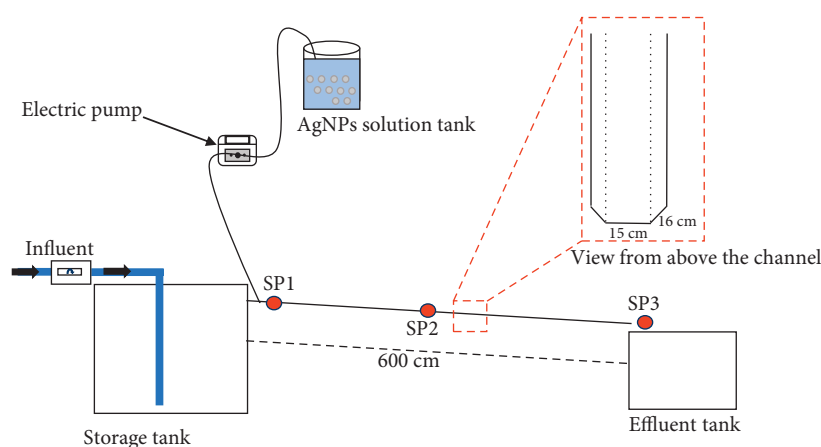


FIGURE 1: Schematic of the simulated river system.

TABLE 2: Design parameters of the simulated river system.

Parameter	Unit	Value
Length of the river	cm	600
River flow	L/min	0.8
AgNP concentration	$\mu\text{g/L}$	17541
Storage tank size	cm ³	$59 \times 43 \times 39$
Experimental period	min	320

dissolved oxygen (DO), total dissolved solids (TDSs), and conductivity during an experiment. The solution of AgNPs with its actual concentration of 17541 $\mu\text{g/L}$ flowed into the simulated river entering at the distance of 10 cm before the SP1 point was adjusted at the flow rate of 0.01 L/min, as shown in Figure 1. The experiment was run under two conditions to monitor the concentration of AgNPs in water over time and to monitor the distribution of Ag sediment on the riverbed at the end of the experiment. A combined flow of tap water and AgNP solution was allowed for 300 min of the experiment, and then, only the tap water flow was allowed for 20 min to inspect the state of AgNPs remained in the water. The concentration of AgNPs in the water was

regularly monitored at three points of SP1 at 10 cm, SP2 at 300 cm, and SP3 at 600 cm of the distance from the point of entry of the AgNP solution into the simulated river, as shown in Figure 1. The procedure of water sampling was performed according to the USEPA 32 grab sampling method. The water samples were collected at a single vertical at the centroid of stream flow and then filled into an empty low-density polyethylene bottle and then stored in an ice cooler box. Then, the water samples were transported to the laboratory and kept in a refrigerator at 4°C. The presence and distribution of the silver sediment on the riverbed were monitored at three sampling points of SP1, SP2, and SP3 at the end of the experiment.

2.5. Characterization and Analytical Techniques. The digestion of a 5 g water sample mixed with 7 mL of HNO₃ (69%) and H₂O₂ (30%) was carried out using the Milestone-START D-Microwave Digestion System with 12 digestion vessels (Milestone Srl, Milan, Italy), operating with the easyCONTROL software at a power of 1000 W, a pressure of 45 bar, and a temperature of 200°C for 15 min, and then cooled for 30 min. Then, the mixture was diluted with Milli-

Q water to 25 mL, and then, the concentration of AgNPs in water was analyzed using the Inductive Coupled Plasma Optical Emission Spectroscopy (Agilent 710 Series ICP-OES, Santa Clara, CA, USA), operating with the ICP-Expert II software at a power of 1200 W and argon flow rate of 15 L/min. The presence and distribution of the Ag sediment on the riverbed was characterized using the Field Emission Scanning Electron Microscope (FESEM Zeiss Supra 35VP, Oberkochen, Baden-Württemberg, Germany) and observed at an accelerating voltage of 5 kV. The elemental analysis of clay soil was carried out using the Scanning Electron Microscopy with Energy Dispersive X-ray (SEM-EDX) analysis (HITACHI S-3400N, Chiyoda-ku, Tokyo, Japan) equipped with the Bruker Quantax software and operated at a voltage of 15 kV.

3. Results and Discussion

3.1. Water Quality Parameters. The results (Figure 2(a)) of monitoring the water temperature during the experiment show that the temporal variation of temperature ranged from 26.9°C to 27.4°C with an average of 27.2°C in the storage tank (see Figure 2(a), line-i) and from 27.1°C to 27.6°C with an average of 27.4°C at outlet of the simulated river (see Figure 2(a), line-ii). The presence of AgNPs in water leading to a very low increase in the temperature of water could be due to that the AgNPs might partially dissolve into Ag^+ in the presence of air causing an increase in the zeta potential value of tap water [18]. The contamination of AgNPs does not induce a significant change in the temperature of water but has a negative effect on the ecological health of aquatic organisms [19]. The pH of water slightly increases from 6.86 to 7.04 in the influent (see Figure 2(b), line-i) and moderately decreases from 7.33 to 7.00 in the effluent (see Figure 2(b), line-ii) of the simulated river with increasing of the operational time from 10 to 90 min of the experiment which could be due to that oxygen dissolved by diffusion from the surrounding air during the flow of water across the simulated river can reduce the pH of water [20]. Then, the pH of water is almost constant at around pH 7.11 in influent and at around pH 7.03 in effluent of the simulated river for a period of 210 min from 90 to 320 min of the experiment (see Figure 2(b)). The pH of the effluent lower than that of the influent could be due to that the dissolution of AgNPs allowed for the reaction of Ag^+ with OH^- from water, which can cause the precipitation of AgOH and may release the H^+ ions to decrease the pH of the effluent [21].

Generally, the DO of the influent ranging from 3.70 to 5.03 mg/L with an average of 4.12 mg/L (see Figure 2(c), line-i) was higher than that of the effluent ranging from 3.18 to 4.46 mg/L with an average of 3.66 mg/L (see Figure 2(c), line-ii) which could be due to that the hydrodynamic sizes of AgNPs influenced by the moving water in the simulated river at conditional random fields can adsorb more oxygen leading to a decrease in the amount of DO in the effluent [22]. The TDS of the influent ranging from 68.9 to 71.5 mg/L with an average of 71.0 mg/L (see Figure 2(d), line-i) was lower than that of the effluent ranging from 75.4 to

78.0 mg/L with an average of 77.3 mg/L (see Figure 2(d), line-ii) which could be due to the presence of AgNPs at a certain concentration in water, and the water flowing through the simulated river contributing to a release of clay mineral particles caused by both chemical dissolution and mechanical deterioration may lead to an increase in the TDS value by 8.2%. The conductivity of the influent ranging from 110.17 to 115.13 $\mu\text{S}/\text{cm}$ with an average of 113.86 $\mu\text{S}/\text{cm}$ (see Figure 2(e), line-i) was lower than that of the effluent ranging from 120.40 to 125.70 $\mu\text{S}/\text{cm}$ with an average of 124.25 $\mu\text{S}/\text{cm}$ (see Figure 2(e), line-ii) which could be due to that the release of Ag^+ ions from AgNPs can lead to an increase in the conductivity of water in the effluent tank by 8.3% [23]. This study revealed that the presence of AgNPs can lead to a slight increase in the temperature of water, a slight decrease in both the pH and DO of the water, and a moderate increase in both the TDS and conductivity of the water.

3.2. AgNPs in Water. The results (Figure 3) of monitoring the AgNP concentration in water show that the patterns of AgNP variation can be divided into three phases, namely, the adaptation phase for a period of 30 min from 0 to 30 min, the steady-state phase for a period of 270 min from 30 to 300 min, and the termination phase for a period of 20 min from 300 to 320 min of the experiment. The concentration of AgNPs monitored at the SP1 sampling point varies from 32.30 to 62.25 $\mu\text{g}/\text{L}$ with an average of 43.66 $\mu\text{g}/\text{L}$ during the adaptation period, then from 136.77 to 193.48 $\mu\text{g}/\text{L}$ with an average of 164.49 $\mu\text{g}/\text{L}$ under a steady-state condition, and from 6.44 to 7.13 $\mu\text{g}/\text{L}$ with an average of 6.67 $\mu\text{g}/\text{L}$ during the termination phase of the experiment (see Figure 3, line-i). The concentration of AgNPs monitored at the SP2 sampling point varies from 108.82 to 149.94 $\mu\text{g}/\text{L}$ with an average of 131.43 $\mu\text{g}/\text{L}$ during the adaptation phase, then from 112.96 to 229.30 $\mu\text{g}/\text{L}$ with an average of 170.02 $\mu\text{g}/\text{L}$ under a steady-state condition, and from 4.28 to 10.04 $\mu\text{g}/\text{L}$ with an average of 7.81 $\mu\text{g}/\text{L}$ during the period of terminating the experiment (see Figure 3, line-ii). The concentration of AgNPs monitored at the SP3 sampling point varies from 166.92 to 200.33 $\mu\text{g}/\text{L}$ with an average of 179.71 $\mu\text{g}/\text{L}$ during the phase of adaptation, then from 156.10 to 286.15 $\mu\text{g}/\text{L}$ with an average of 221.35 $\mu\text{g}/\text{L}$ under a steady-state condition, and from 7.13 to 14.17 $\mu\text{g}/\text{L}$ with an average of 9.78 $\mu\text{g}/\text{L}$ during the experimental termination period (see Figure 3, line-iii).

The rapid spread of AgNPs deposited on the riverbed at the sampling points of SP1 and SP2 could be due to the physicochemical interactions between AgNPs and clay particles, which depend on the active sites of clay minerals and the nature of Ag species [24] and may lead to a decrease in the concentration of AgNPs in water during the first 5 min of the experiment. The physicochemical interactions of AgNPs with clay soil surfaces could be efficient in retaining the AgNPs material on the riverbed along the simulated river [25], and the dispersion interaction may associate with the nature of clay adsorbent [26]. The spread of silver sediment on the surface of clay soil at the downstream part of the simulated river may take a long time until 10 min of the

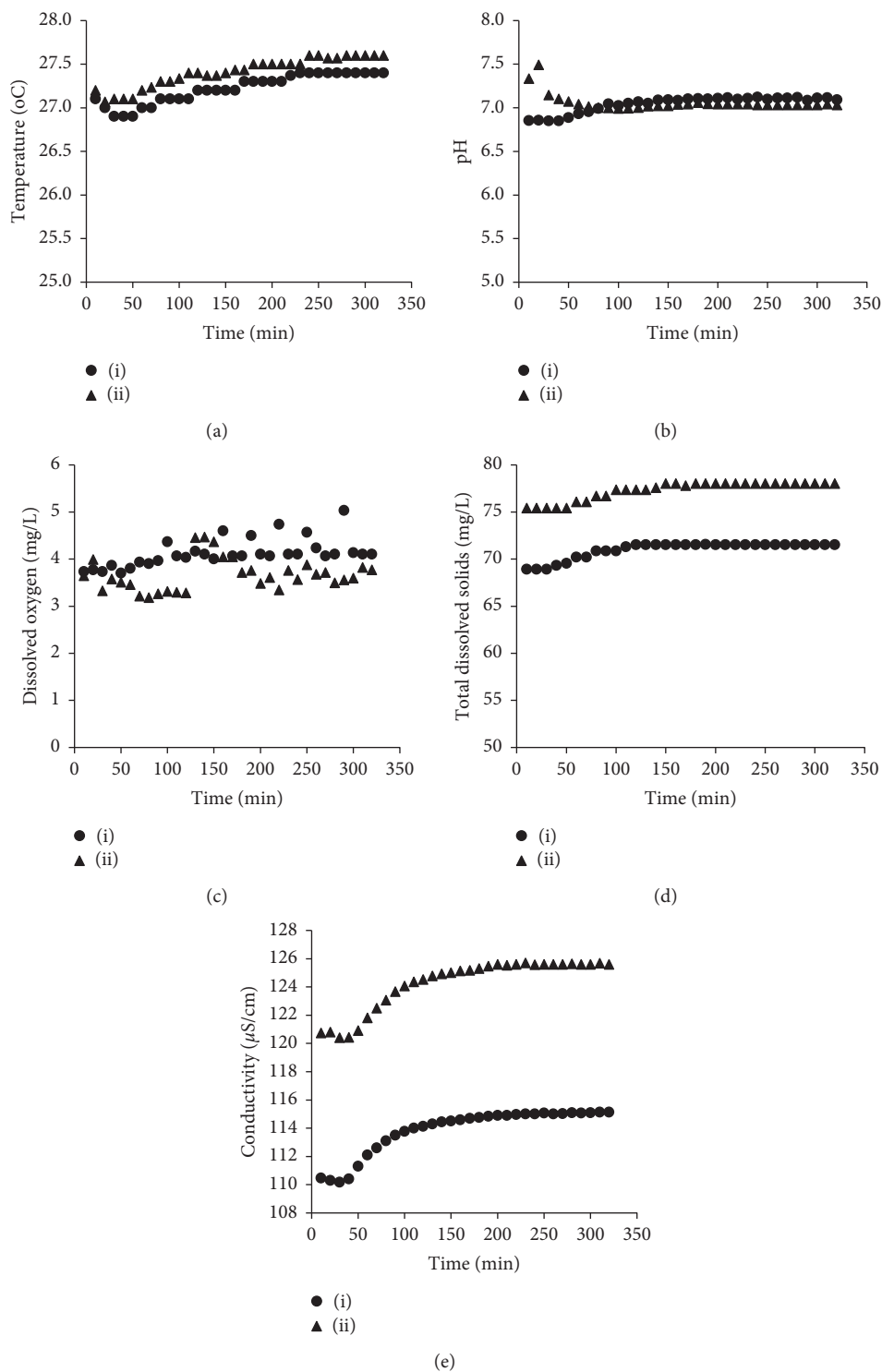


FIGURE 2: Variation of (a) temperature, (b) pH, (c) dissolved oxygen, (d) total dissolved solids, and (e) conductivity monitored at the (i) influent and (ii) effluent of the simulated river.

experiment because the elemental content of Ag in water progressively reduces during the transportation of AgNPs until reaching at the sampling point of SP3. The average concentration of AgNPs in water under a steady-state condition increases from 164.49 to 170.02 and then to 221.35 $\mu\text{g}/\text{L}$ with an increase of the channel length from 10 to

300 and then to 600 cm at the downstream location of the entry of the AgNP solution into the water body. This could be due to that the accumulation of Ag sediment released from clay soil at the bottom of the simulated river may lead to an increase in the concentration of AgNPs in water [24]. The variation of AgNP concentration under a steady-state

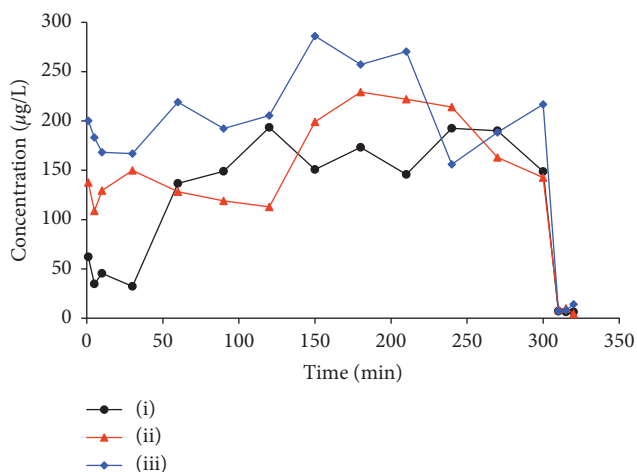


FIGURE 3: Variations of AgNPs monitored at the sampling points of (i) SP1 at 10 cm, (ii) SP2 at 300 cm, and (iii) SP3 at 600 cm from the point of entry of the AgNP solution into the water body.

condition could be due to that the fate and behaviors of AgNPs affected by a combined process of sedimentation, aggregation, and dissolution may occur over time during the transport of AgNPs across the simulated river [27]. The future studies can help to define the importance of aggregation effects on the transport and risk of AgNPs in the environment and contribute to an advance in the understanding of many variables affected by adhesion strength between AgNPs and clay particles [28, 29].

3.3. AgNP Distribution. The FESEM images and EDX mapping analysis (Figure 4) of AgNPs freely dispersed on the surface of clay soil were monitored at the sampling points of SP1, SP2, and SP3 along the simulated river. The FESEM images of Figures 4(a)–4(c)- (i) show the spread of AgNPs to confirm the presence of Ag sediment deposited on the riverbed. The EDX mapping analysis of Figures 4(a)–4(c)- (ii) shows that the distribution of Ag sediment is dispersed on the entire surface of clay soil. Even though the division of AgNPs adsorbed to the wastewater biosolids can be found in the sludge and effluent of the WWTP process, the transmission electron microscopy analysis of AgNP distribution was confirmed to freely disperse in the effluent [13]. The distribution of Ag sediment on the surface of clay soil under the weathering conditions of wastewater can have a most dramatic effect on the transformation of AgNPs into AgCl and Ag₂S [30]. The mechanisms of Ag sediment trapped onto the riverbed during the transport of AgNPs by the water flow include the physicochemical interactions, gravity force, and water flow rate. Understanding the distribution, translocation, and accumulation of Ag species trapped on the clay soil along the river by modeling the elemental content of Ag may help guide the future investigation due to that the environmental impact of AgNPs on the aquatic biota may vary significantly as a function of the river length, water flow rate, and trapped distribution model of Ag sediment.

3.4. AgNPs in Soil. The results (Table 3) of the SEM-EDX analysis show that the elemental contents of oxygen, aluminium, silicon, potassium, iron, and silver in clay soil are as high as 53.29%, 19.36%, 22.26%, 0.58%, 4.51%, and 0.00%, respectively. Oxygen, silicon, and aluminium are notably the most common elements contained in clay soil [31], while it does not seem to contain silver before feeding the AgNP solution. The contents of silver in clay soil as high as 0.30%, 0.39%, and 0.47% were verified at the sampling point locations of SP1, SP2, and SP3, respectively, after feeding the AgNP solution into the water flow. An increase in the content of silver from the upstream to downstream area of the simulated river could be due to that the probability of clay soil trapped silver is more favorable for AgNP gravity in the downstream part of the simulated river [32]. The physicochemical interactions of AgNPs with clay soil particles can help retain more silver in the downstream part of the simulated river even when organic material was absent [25]. A small content of Ag sediment trapped in clay soil has not significantly changed in the percent major elemental compositions of oxygen, aluminium, and silicon along the simulated river.

The discharge of AgNP material into the simulated river can be divided into two fractions. The fraction of AgNPs dissolved in water flowing from the upstream to downstream area of the simulated river can be verified from the variations of AgNP concentration at different sampling points over time (see Figure 3). The fraction of AgNP gravity deposited on the riverbed as Ag sediment can be verified from the elemental content of Ag along the simulated river (see Table 3), while the sedimentation of silver on the riverbed drives the removal of AgNPs from the water channel [33]. By considering the actual amount of AgNPs in water is at the concentration of 17541 µg/L, the percentage of the average concentration of AgNPs remained in water increased by 0.94% from 17541 to 164.49 µg/L, by 0.97% from 17541 to 170.02 µg/L, and by 1.26% from 17541 to 221.35 µg/L with an increase of the channel distance by 10 cm from 0 to 10 cm, by 90 cm from 10 to 300 cm, and by 300 cm from 300 to 600 cm, respectively, from the point of discharge of AgNPs into the simulated river. The continuous flow of water can push the settled AgNP material on the clay soil surface moving towards the downstream area of the simulated river leading to an increase in the sedimentation of Ag species [27]. It is possible to carry the settled AgNP material towards the downstream area of the simulated river by gravity force because the simulated river system designed with a slope of 5.7° aims to mimic the natural flow of water in a river. This study provides a new insight into the natural process of AgNP transportation along the river.

3.5. Implication for Future Research. The transport models of AgNPs can determine the large fraction of silver remained in the sludge and liquid phase of wastewater flowed along an effluent channel causing the transformation of AgNPs to Ag₂S [13, 34]. More than 90% of AgNPs that remained in the effluent of WWTP indicate the majority of Ag species passing through the subsequent treatment units of WWTP,

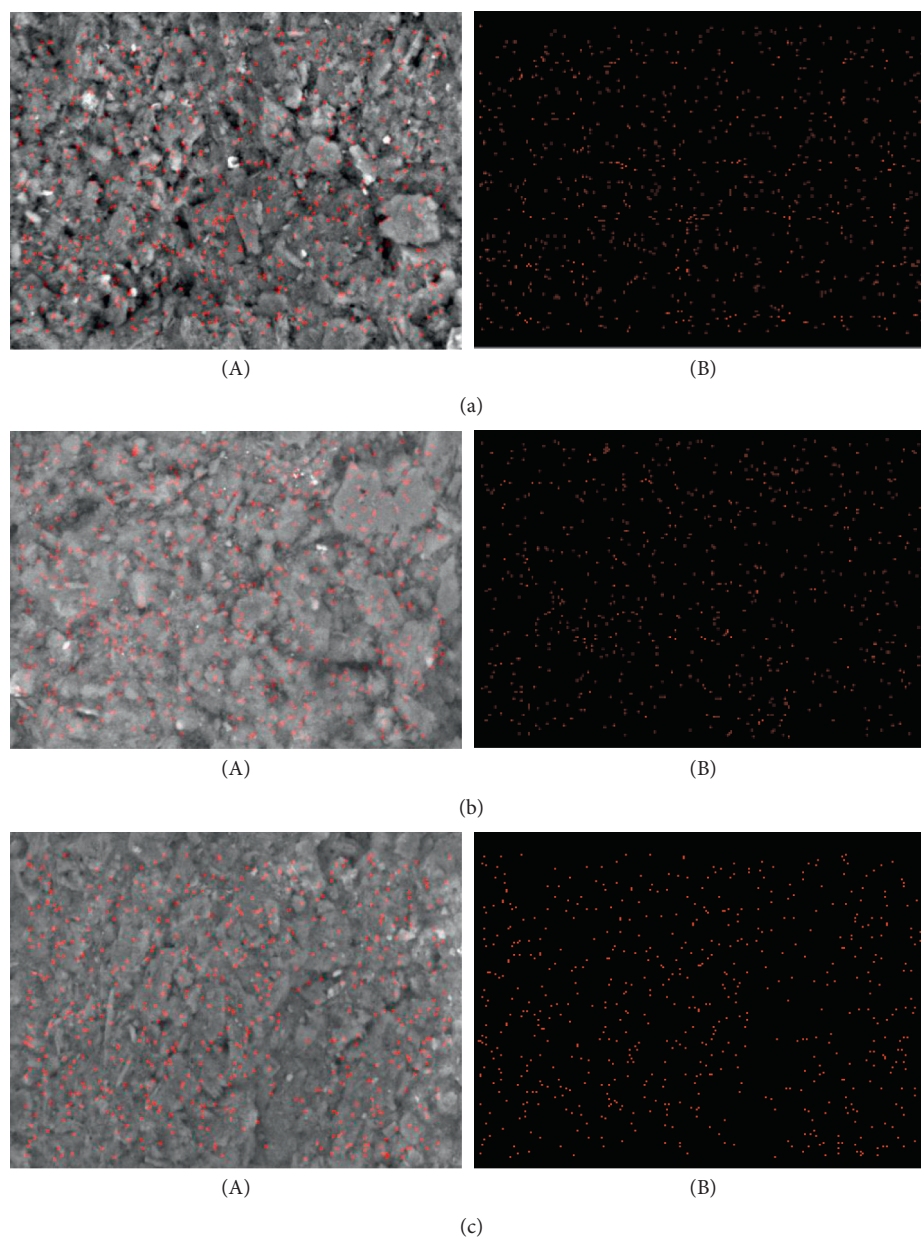


FIGURE 4: Distribution of AgNPs monitored at the sampling points of (a) SP1 at 10 cm, (b) SP2 at 300 cm, and (c) SP3 at 600 cm from the point of entry of the AgNP solution released to the water body with (i) the FESEM image and (ii) the EDX mapping analysis.

TABLE 3: Elemental analysis of clay soil at different sampling points.

Element	Content of the elements in clay soil (%)			
	Original clay soil	SP1 sampling point	SP2 sampling point	SP3 sampling point
Oxygen	53.29	55.17	51.26	55.11
Aluminium	19.36	18.72	19.87	19.14
Silicon	22.26	20.86	22.81	21.01
Potassium	0.58	0.45	0.43	1.25
Iron	4.51	4.50	5.24	3.02
Silver	0.00	0.30	0.39	0.47
Total	100.00	100.00	100.00	100.00

and this may limit the use of the treated wastewater as an agricultural fertilizer [12, 14]. The results of this study indicate the actual amount of 17541 $\mu\text{g/L}$ AgNPs entered tap water at a flow rate of 0.01 L/min from which only approximately 1.26% (or 221.35 $\mu\text{g/L}$) of AgNPs can remain in the water flow at the SP3 sampling point of the simulated river. An investigation of the contradictory results is due to that the simulated river system designed to mimic the natural flow of a river is different from the effluent channel of WWTP. A previous study reported that approximately 90–99% of AgNPs entered the WWTP facilities which can accumulate in the biosolids of activated sludge and sludge cake [15]. The development of new models in the future may facilitate a better understanding of the retention and mobility mechanisms of the AgNP material under complicated environmental conditions. This study suggested that the variables of slope, water flow rate, feeding rate of the AgNP solution, sampling location, and soil type must be considered for studying the transport mechanisms of AgNP material through either the natural flow of a river or the effluent channel of the WWTP processes.

4. Conclusions

This study used the simulated river to investigate the fate and transport of AgNPs dispersed along the water flow. The amount of AgNPs remained in water flow could be very low depending on the distance from the solution of AgNPs discharged into the water body to an observed location along the simulated river. The FESEM images and EDX mapping analysis show the elemental content of Ag freely dispersed across the riverbed depending on the distance of observed location to the solution of AgNPs entered the water body. The results of this study can be used as the basis for future research to fully investigate the fate and transport of AgNPs dispersed by water flow in the environment.

Data Availability

Data are available on request to achmadsyafiuddin@unusa.ac.id.

Conflicts of Interest

The authors declare no conflicts of interest regarding the publication of this paper.

Acknowledgments

The authors thank Mohd Azlan and Tasnia Hassan Nazifa for their technical assistance during the experiment. Mu. Naushad is grateful to the Researchers Supporting Project Number (RSP-2021/8), King Saud University, Riyadh, Saudi Arabia, for the financial support. The authors gratefully acknowledge the financial support from the Universiti Teknologi Malaysia for the project COE for Contract No. QJ130000.2422.04G06 and the project GUP for Contract No. QJ130000.2522.18H92. The authors also thank the Universitas Nahdlatul Ulama Surabaya for facilitating this work under Contact Nos. 161.3/UNUSA/Adm-LPPM/III/

2021, 161.4/UNUSA/Adm-LPPM/III/2021, and 161.5/UNUSA/Adm-LPPM/III/2021.

References

- [1] C. O. Hendren, A. R. Badireddy, E. Casman, and M. R. Wiesner, "Modeling nanomaterial fate in wastewater treatment: Monte Carlo simulation of silver nanoparticles (nano-Ag)," *The Science of the Total Environment*, vol. 449, pp. 418–425, 2013.
- [2] X.-F. Zhang, Z.-G. Liu, W. Shen, and S. Gurunathan, "Silver nanoparticles: synthesis, characterization, properties, applications, and therapeutic approaches," *International Journal of Molecular Sciences*, vol. 17, no. 9, p. 1534, 2016.
- [3] F. Esmail, H. Koohestani, and H. Abdollah-Pour, "Characterization and antibacterial activity of silver nanoparticles green synthesized using *Ziziphora clinopodioides* extract," *Environmental Nanotechnology, Monitoring & Management*, vol. 14, p. 100303, 2020.
- [4] P. M. Potter, J. Navratilova, K. R. Rogers, and S. R. Al-Abed, "Transformation of silver nanoparticle consumer products during simulated usage and disposal," *Environmental Sciences: Nano*, vol. 6, no. 2, pp. 592–598, 2019.
- [5] J. E. Choi, S. Kim, J. H. Ahn et al., "Induction of oxidative stress and apoptosis by silver nanoparticles in the liver of adult zebrafish," *Aquatic Toxicology*, vol. 100, no. 2, pp. 151–159, 2010.
- [6] P. R. Cáceres-Vélez, M. L. Fascineli, E. Rojas et al., "Impact of humic acid on the persistence, biological fate and toxicity of silver nanoparticles: a study in adult zebrafish," *Environmental Nanotechnology, Monitoring & Management*, vol. 12, p. 100234, 2019.
- [7] K. Bilberg, H. Malte, T. Wang, and E. Baatrup, "Silver nanoparticles and silver nitrate cause respiratory stress in Eurasian perch (*Perca fluviatilis*)," *Aquatic Toxicology*, vol. 96, no. 2, pp. 159–165, 2010.
- [8] T. M. Scown, E. M. Santos, B. D. Johnston et al., "Effects of aqueous exposure to silver nanoparticles of different sizes in rainbow trout," *Toxicological Sciences*, vol. 115, no. 2, pp. 521–534, 2010.
- [9] M. Afifi, S. Saddick, and O. A. Abu Zinada, "Toxicity of silver nanoparticles on the brain of *Oreochromis niloticus* and *Tilapia zillii*," *Saudi Journal of Biological Sciences*, vol. 23, no. 6, pp. 754–760, 2016.
- [10] A. Ale, A. S. Rossi, C. Bacchetta, S. Gervasio, F. R. De La Torre, and J. Cazenave, "Integrative assessment of silver nanoparticles toxicity in *Prochilodus lineatus* fish," *Ecological Indicators*, vol. 93, pp. 1190–1198, 2018.
- [11] S.-J. Yu, Y.-G. Yin, and J.-F. Liu, "Silver nanoparticles in the environment," *Environmental Sciences: Processes Impacts*, vol. 15, no. 1, pp. 78–92, 2013.
- [12] T. M. Benn and P. Westerhoff, "Nanoparticle silver released into water from commercially available sock fabrics," *Environmental Science & Technology*, vol. 42, no. 11, pp. 4133–4139, 2008.
- [13] R. Kaegi, A. Voegelin, B. Sinnet et al., "Behavior of metallic silver nanoparticles in a pilot wastewater treatment plant," *Environmental Science & Technology*, vol. 45, no. 9, pp. 3902–3908, 2011.
- [14] L. Hou, K. Li, Y. Ding et al., "Removal of silver nanoparticles in simulated wastewater treatment processes and its impact on COD and NH₄ reduction," *Chemosphere*, vol. 87, no. 3, pp. 248–252, 2012.

- [15] Y. Kim, "Nanowastes treatment in environmental media," *Environmental Health and Toxicology*, vol. 29, p. e2014015, 2014.
- [16] K. B. Riaz Ahmed, A. M. Nagy, R. P. Brown, Q. Zhang, S. G. Malghan, and P. L. Goering, "Silver nanoparticles: significance of physicochemical properties and assay interference on the interpretation of in vitro cytotoxicity studies," *Toxicology in Vitro*, vol. 38, pp. 179–192, 2017.
- [17] K. N. M. Mahdi, R. Peters, M. Van Der Ploeg, C. Ritsema, and V. Geissen, "Tracking the transport of silver nanoparticles in soil: a saturated column experiment," *Water, Air, & Soil Pollution*, vol. 229, no. 10, p. 334, 2018.
- [18] K. Loza, J. Diendorf, C. Sengstock et al., "The dissolution and biological effects of silver nanoparticles in biological media," *Journal of Materials Chemistry B*, vol. 2, no. 12, pp. 1634–1643, 2014.
- [19] T.-L. Pham, "Effect of silver nanoparticles on tropical freshwater and marine microalgae," *Journal of Chemistry*, vol. 2019, Article ID 9658386, 7 pages, 2019.
- [20] M. Radwan, P. Willems, A. El-Sadek, and J. Berlamont, "Modelling of dissolved oxygen and biochemical oxygen demand in river water using a detailed and a simplified model," *International Journal of River Basin Management*, vol. 1, no. 2, pp. 97–103, 2003.
- [21] B. Molleman and T. Hiemstra, "Time, pH, and size dependency of silver nanoparticle dissolution: the road to equilibrium," *Environmental Sciences: Nano*, vol. 4, no. 6, pp. 1314–1327, 2017.
- [22] W. Zhang, Y. Yao, K. Li, Y. Huang, and Y. Chen, "Influence of dissolved oxygen on aggregation kinetics of citrate-coated silver nanoparticles," *Environmental Pollution*, vol. 159, no. 12, pp. 3757–3762, 2011.
- [23] G. A. Sotiriou, A. Meyer, J. T. N. Knijnenburg, S. Panke, and S. E. Pratsinis, "Quantifying the origin of released Ag⁺ ions from nanosilver," *Langmuir*, vol. 28, no. 45, pp. 15929–15936, 2012.
- [24] J. Kyziol-Komosinska, A. Dzieniszewska, W. Franus, and G. Rzepa, "Behavior of Ag species in presence of aquatic sediment minerals-in context of aquatic environmental safety," *Journal of Contaminant Hydrology*, vol. 232, p. 103606, 2020.
- [25] L. Degenkolb, F. Leuther, S. Lüderwald et al., "The fate of silver nanoparticles in riverbank filtration systems - the role of biological components and flow velocity," *The Science of the Total Environment*, vol. 699, p. 134387, 2020.
- [26] M. A. Fulazzaky, "Study of the dispersion and specific interactions affected by chemical functions of the granular activated carbons," *Environmental Nanotechnology, Monitoring & Management*, vol. 12, p. 100230, 2019.
- [27] L.-J. A. Ellis, M. Baalousha, E. Valsami-Jones, and J. R. Lead, "Seasonal variability of natural water chemistry affects the fate and behaviour of silver nanoparticles," *Chemosphere*, vol. 191, pp. 616–625, 2018.
- [28] M. A. Fulazzaky, M. Fulazzaky, and K. Sumeru, "Evaluation of coating rate and adhesive force for copper deposition on the surface of polypropylene," *Journal of Adhesion Science and Technology*, vol. 33, no. 13, pp. 1438–1452, 2019.
- [29] E. M. Hotze, T. Phenrat, and G. V. Lowry, "Nanoparticle aggregation: challenges to understanding transport and reactivity in the environment," *Journal of Environmental Quality*, vol. 39, no. 6, pp. 1909–1924, 2010.
- [30] S. Mohan, J. Princz, B. Ormeci, and M. C. DeRosa, "Morphological transformation of silver nanoparticles from commercial products: modeling from product incorporation, Weathering through Use Scenarios, and Leaching into Wastewater," *Nanomaterials*, vol. 9, no. 9, p. 1258, 2019.
- [31] Y. N. Vodyanitskii, "Elements oxides as a source of errors in the gross chemical composition of soil and ways to eliminate the errors," *Annals of Agrarian Science*, vol. 16, no. 1, pp. 90–93, 2018.
- [32] O. Sagee, I. Dror, and B. Berkowitz, "Transport of silver nanoparticles (AgNPs) in soil," *Chemosphere*, vol. 88, no. 5, pp. 670–675, 2012.
- [33] I. Velzeboer, J. T. K. Quik, D. van de Meent, and A. A. Koelmans, "Rapid settling of nanoparticles due to heteroaggregation with suspended sediment," *Environmental Toxicology & Chemistry*, vol. 33, no. 8, pp. 1766–1773, 2014.
- [34] T. Y. Sun, F. Gottschalk, K. Hungerbühler, and B. Nowack, "Comprehensive probabilistic modelling of environmental emissions of engineered nanomaterials," *Environmental Pollution*, vol. 185, pp. 69–76, 2014.